

# EEG-based Recognition of Driver State Related to Situation Awareness Using Graph Convolutional Networks

Ruilin Li  
Fraunhofer Singapore  
Nanyang Technological University  
Singapore  
Ruilin001@e.ntu.edu.sg

Zirui Lan  
Fraunhofer Singapore  
Singapore  
Lan.Zirui@fraunhofer.sg

Jian Cui  
Fraunhofer Singapore  
Nanyang Technological University  
Singapore  
Cuijian@ntu.edu.sg

Olga Sourina  
Fraunhofer Singapore  
Nanyang Technological University  
Singapore  
EOSourina@ntu.edu.sg

Lipo Wang  
School of Electrical and Electronic Engineering  
Nanyang Technological University  
Singapore  
ELPWang@ntu.edu.sg

**Abstract**—Extracting intra- and inter- subject parameters from Electroencephalogram (EEG) representing different Situation Awareness (SA) status is a critical challenge for objective SA recognition. Most of the existing work focuses on the subject-dependent classification that applies power spectrum density (PSD) features. In this paper, we propose a novel spectral-spatial (S-S) model for cross-subject fatigue-related SA recognition. The S-S model not only considers the biological topology across different brain regions to capture both local and global relations among different EEG channels, but also extracts spectral features for each EEG channel. Specifically, we firstly model the topological structure of EEG channels via an adjacency matrix which is built based on the Euclidean distance between EEG channels. Then, the graph convolution operation is employed to perform the neighbourhood aggregation for extracting spatial features. We test our model on a public dataset collected during driver’s task performance. The subject-independent performance of the model is explored. Results demonstrate (1) the superior performance of our model compared with the state-of-the-art models on SA recognition from EEG signals. Specifically, our S-S model achieves 70.6% accuracy which is higher than traditional machine learning methods by 2.7%-6.8% and deep learning methods by 10.3%-11.6%; (2) EEG signal at the occipital region can better reflect the change of SA.

**Keywords**—Situation awareness recognition; Graph Convolution Networks; EEG

## I. INTRODUCTION

A driver needs to maintain a good situation awareness (SA) to track the dynamic, changing road situation efficiently and keep safe driving. Current driver situation awareness research mainly focuses on the analysis of the secondary task [1] and fatigue [2] effects on driver’s SA in normal and automated driving. However, little is known about the progression of measuring driver’s SA. This paper works on the assessment of driver fatigue-related SA.

Situation awareness (SA) is defined as “the perception of the elements in the environment within a volume of time and space, the comprehension of their meaning, and the projection of their status in the near future” [3]. Specifically, SA concerns the knowledge of a person’s complex operating environments. Up to now, there are six approaches to measuring SA [4], such as the freeze-probe technique (SAGAT) [5] and a real-time probe technique (SPAM) [6]. Although these techniques can measure the SA to some extent, the problems of intrusiveness and non-objectiveness cannot be ignored. In our study, we utilize the physiological signals to evaluate SA, which can better solve the mentioned problems. Situation awareness is a cognitive behaviour that is related to our brain activity. Among various signals, electroencephalogram (EEG) is one of the most commonly used signals to record brain activity [7]. Therefore, EEG signals play a crucial role in SA, which can reflect SA more directly.

Some attempts on SA recognition using EEG have been done in other areas such as aviation [8]. The existing EEG-based SA recognition methods are primarily based on traditional supervised machine learning approaches trained on the extracted power spectrum density (PSD) features. Although the PSD features plays an important role in subject-dependent SA recognition, for the subject-independent classification, better classifier and more discriminative EEG representations should be explored. Compared with the traditional methods which only extract spectral features, deep learning methods can learn complex information from multiple dimensions simultaneously [9]. However, one aspect of EEGs that make both traditional and deep learning methods difficult to analyse is the structure of channels placed on an EEG headset. For the traditional methods, the spatial information is usually not be considered. For the deep learning methods, most of the existed investigation just applies the convolution layer to extract the spatial feature but not considers the real connection relationship between EEG channels. By referencing the deep learning algorithm applied in the

recognition of other mental states, it can be found that the common model architectures cannot completely solve the spatial problem. Therefore, for the purpose of extracting spatial features based on the real neighbourhood relationship of EEG channels, we model the 3D EEG channels in a graph structure.

In this paper, we propose a spectral-spatial model aiming to address the aforementioned challenges. This model differs from the common deep learning method by exploiting the topological structure of the EEG channels. The key novelty of this work is that the model utilizes the spectral feature and spatial feature together to assess subject-independent SA. The main contributions are listed as follows:

- A spectral-spatial model is proposed to address the fatigue-related SA recognition problem in inter-subject.
- Model the topological structure of EEG channels.
- Perform spatial localization of SA in the brain.

The following parts of this paper are organized as follows. Section II reviews the related work. Section III describes the dataset we used and the proposed model. Section IV presents the experiment results. Section V concludes the whole paper.

## II. RELATED WORKS

### A. Situation awareness and fatigue

Fatigue can impact the driver's situation awareness. Improvements in vigilance and the avoidance of fatigue and distraction can have a direct impact on SA [10]. Since the effective management of the operators' information acquired from the environment is extremely critical for situation awareness, it is important to avoid attentional narrowing and negligence of important information and tasks, that is, operators need to keep good vigilance during the operation, which is the foundation of a good SA. When the operator lacks vigilance, he/she may neglect to monitor the instruments' parameters, resulting in significant reductions in situation awareness [11]. Some study on fatigue recognition have been done [12]. In this work, based on the different fatigue state of drivers, the two states of SA are defined.

### B. Situation awareness measurement from EEG signal

Raul Fernandez Rojas et al. [13] used LDA algorithm to recognize four SA levels (defined by four different teleoperation conditions). Their preliminary results offered evidence for the potential use of EEG to offer real-time indicators for the objective assessment of SA. Some other previous attempts to measure SA using EEG are limited and have shown diverse results. Catherwood et al. [14], used electroencephalography (EEG) to map brain activity during loss of situation awareness to identify target patterns and threats in urban scenes; their results showed that loss of situation awareness activated cortical areas associated with cognition, such as prefrontal, anterior cingulate, parietal, and visual regions. Yeo et al. [15] used EEG to monitor SA in an air traffic controller (ATC) task. Their model predicted the response latency of the ATC operators with a 10% error. French et al. [16] adopted Endsley's model of SA and

label three levels of SA with different presentation of stimuli. Following, based on the power spectral density (PSD), the SA classification is performed with poor accuracy. In a different study, Berka et al. [17] also used events related to Endsley's levels of SA. They compared event-related potentials (ERPs) and the PSD (1) between moments of correct and incorrect target identification, and (2) between reading questions and reading information. Although they distinguished bad SA from good, the problem is that these events cannot be extracted in real-time. Vidulich et al. [18] took a completely different approach that is more consistent with the perceptual cycle model. They manipulated the display in a target-identification task to more or less facilitate target identification. PSD was also used in their work. Results showed that theta power (4-7 Hz) was higher and alpha power (8-14 Hz) was lower in many channels in the most difficult conditions compared to easier conditions, which is consistent with higher attentional demands. Unfortunately, the paper was not able to determine the task difficulty that affected the quality of SA, limiting the implications of their results.

### C. Graph neural network

In the EEG-based recognition problems, the performance of deep convolutional neural networks (CNN) and recurrent neural networks (RNN) are superior to the traditional EEG analysis methods [19, 20]. However, the traditional CNN that can obtain local spatial features can only be used in Euclidean space, such as images and a regular grid, etc. The actual topological structure of EEG electrodes is complex, and the CNN cannot clearly reflect it. In this work, we model the EEG electrodes in the form of graph. Recently, applying graph neural network (GNN) to handle different kinds of graph-structured data, especially generalizing the CNN to the graph convolution network (GCN) [21], has been successfully applied in many applications, including document classification [22] and transportation prediction [23], etc.

In 2009, Scarselli first proposed the concept of graph convolution neural network (GCNN) [24], which is a class of neural networks that are derived from CNN and spectral theory [25]. Zhong, et al [26] performed EEG-based emotion recognition using regularized GNN. They proposed node-wise domain adversarial training and emotion-aware distribution learning (EmotionDL). These two regularizers can help to improve the robustness of the model against the EEG variations and noisy labels. The adjacency matrix they used is:  $A_{ij} = \exp(-\frac{d_{ij}}{2\delta^2})$ , which is based on the Salvador's theory that the strength of connection between brain regions decays as an inverse square or gravity-law function of physical distance [27], where  $d$  denotes the physical distance. Regarding the adjacency matrix. Wang et al. [28] proposed phase-locking value (PLV) based GCNN (P-GCNN) for emotion recognition, in which the phase information is considered to be useful and the adjacency matrix is defined based on PLV. The P-GCNN uses the PLV connectivity of EEG signals to determine the mode of emotional-related functional connectivity. However, the temporal feature of the EEG signal is not used for EEG-based recognition. Covert et al [29] find this

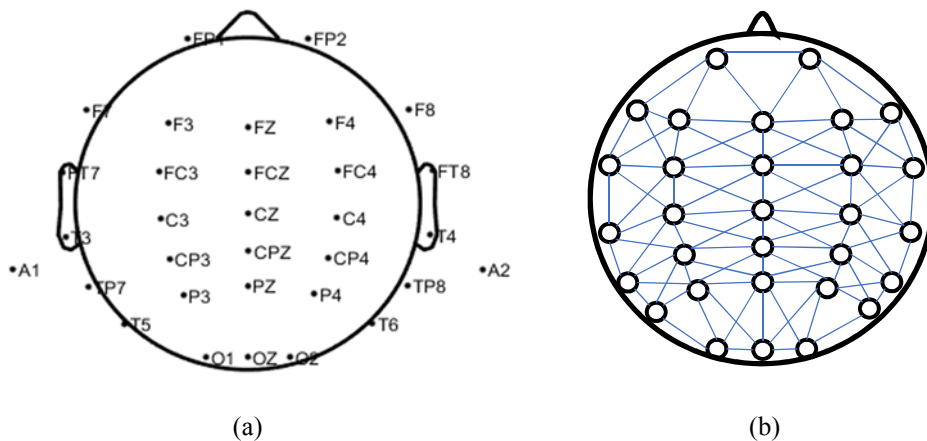


Figure 1. EEG channels. (a) indicates the EEG channel location by name. (b) shows the modelled topological structure. The solid line represents that the two connected nodes are 1-step neighbours.

challenge that the commonly used deep learning models cannot leverage structural and temporal information simultaneously and are not proper for time-series signal. Thus, they proposed the temporal graph neural network for automatic seizure detection. In each layer, the temporal information is extracted by convolution, followed by the aggregation of EEG nodes signals. The parameters in TGCN are shared over both time and space. In this paper, we employ graph convolution network (GCN) to extract spatial information in EEG signals and model the EEG channels based on an adjacency matrix.

### III. MATERIALS AND METHODS

#### A. Data description

We use an open driving dataset in our experiments, which is collected during 2005-2012 and released in 2019 by Cao et al. [30]. The dataset comprises 62 EEG datasets of 27 subjects (aged between 22-28) who were students or staff from National Chiao Tung University.

The EEG data were collected when participants drove and maintained a car in the centre of the lane. During the experiment, lane-departure events were randomly introduced every 6-10 seconds, which made the car drift to left or right from the centre of the lane. The participants were asked to steer the wheel as quickly as possible to move back to the centre of the lane when the lane departure events happened. The deviation onset, movement onset and movement offset were logged, which are the start time of lane-departure event, start time of participants' response to the event and the time point the car moves back to the course were respectively. For inducing the fatigue state of participants, the experiment started after lunch and lasted for approximately 90 minutes.

The EEG signal was recorded in 32 channels (30 valid channels plus 2 reference channels) using Quik-Cap (NeuroScan), which is at a sampling frequency of 500Hz.

#### B. Data preparation

The pre-processed dataset is used in our study. The dataset has been pre-processed by the authors in the

following ways. (1) The raw EEG signals were filtered by 1-Hz high-pass and 50-Hz low pass finite impulse (FIR) filters. (2) Apparent eye blinks that contaminate the EEG signals were manually removed through visual inspection. (3) Ocular and muscular artefacts were removed by the Automatic Artifact Removal (AAR) plug-in in EEGLAB. We further down-sample the data to 128Hz.

In our study, the fatigue-related SA is analysed. Thus, SA is defined qualitatively as fatigue corresponds to poor SA while alert corresponds to good SA, the rest of the data reflects the neutral state. Considering that fatigue and drowsiness can impact the status of SA in disturbing ways, we extract 3 seconds EEG data prior to the deviation onset on the basis that the measurement result of the trial can reflect the subject's SA before the start of the trial. Since the subjects' states cannot be specified before the movement onset, that is, the data may mix both good and poor SA, we did not use the EEG data between deviation onset point and movement onset point. We apply the method described in [30] to extract the fatigue-related SA. Specifically, SA is quantitatively defined based on the reaction time (RT), which is the length of the interval between the deviation onset and movement onset. Additionally, global RT was defined as the average of local RTs across all epochs within a 90-second window before the deviation onset. The baseline alert-RT was defined as the 5<sup>th</sup> percentile of local RT in the entire session. Label process is: When both the local and global RT are shorter than 1.5 times the alert-RT, the corresponding extracted EEG data is labelled as "poor SA", and when both the local and global RT are longer than 2.5 times the alert-RT, the data is labelled as "good SA". Transitional states with moderate performance are excluded and the neutral state is not considered in this work. To ensure sufficient samples of data for training the model, we filtered the datasets such that dataset of each subject should have at least 50 samples of both states. For the subjects that have multiple datasets, we select the most balanced one to perform the filter operation. Finally, we got a whole balanced SA dataset which includes 11 subjects' 1674 samples data. And the data size of one sample was 30 (channels)  $\times$  384 (sample

points). The number of samples for each subject is shown in Table I.

TABLE I. SITUATION AWARENESS DATASET CONTENT

Subject ID	Number of Samples	
	Good SA	Poor SA
1	94	94
5	66	66
22	75	75
31	74	74
35	85	85
41	83	83
42	51	51
43	70	70
44	72	72
45	54	54
53	113	113
Total	837	837

### C. Feature extraction

The spectral band power features are extracted from each EEG segment, which were widely used in SA recognition studies [13, 17, 18]. The power spectral density (PSD) is extracted from these three spectral bands: theta (4-8 Hz), alpha (8-12 Hz), beta (12-30 Hz). Finally, the shape of each sample is  $30 \times 3$ .

### D. Our Spectral-spatial model

The spatial information is extracted by graph convolution layer. The specific process of modelling the EEG electrodes as graph structure and extract the spatial dependence is presented in the following.

Firstly, we model the EEG channels topological structure. In EEG signal collection system, given a group of EEG electrodes  $I \triangleq \{i\}_{1:n}$ , where  $n$  denotes the number of EEG nodes on the graph structure. Based on the Euclidean distance  $d_{ij}$ ,  $i, j = 1, 2, \dots, n$ , computed from the Cartesian coordinate value of channels in EEGLAB “channel location info”, a distance threshold is set that can make every node be connected with its nearest, as shown in Figure 1. If the distance of two channels  $i, j$  is smaller than the threshold, we set the adjacency matrix  $A_{ij} = 1$ . Otherwise,  $A_{ij} = 0$ . Then, we obtain the adjacency matrix  $A \in \mathbb{R}^{n \times n}$  which represents the EEG channels topological structure. Here, we only set the weight of the connection between one node and its nearest neighbourhood nodes as “1”, which

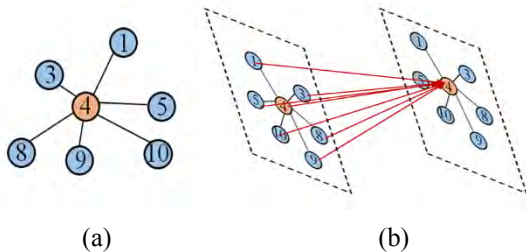


Figure 2. Aggregation operation. (a) is the part of EEG channels topology. The blue nodes indicate the neighbourhood nodes of node 4. (b) We obtain the spatial feature by performing aggregation on node 4 and its neighbouring nodes.

indicates that the information of one node can only spread one step.

Secondly, we extract the EEG channels spatial dependence. The EEG electrodes structure is shown in Figure 1(a). The key challenge for designing the convolution operation to extract spatial information is the different number of neighbours at each node. GNN can manage the similar obstacle by using neighbourhood aggregation schemes [21, 31, 32]. In our system, aggregation is performed across the node  $i$  and its neighbours (figure 2). The process of layer  $l$  can be formulated as follows:

$$s_i^l = \text{AGGREGATE}(\{h_i^{l-1}, \forall i \in N(i)\}), \quad (1)$$

where  $N(i)$  is the set of neighbourhood nodes of node  $i$ , which is defined by the adjacency matrix,  $h_i^l$  is the feature vector of node  $i$  in the layer  $l$  and  $s_i^l$  is the intermediate feature vectors of node  $i$  in the layer  $l$ .

In our work, we employ the convolution operation to aggregate the neighbouring features of node  $i$ . The specific derivation procedure is described in [31]. The output features of layer  $l$  are obtained by:

$$H^l = \sigma(\bar{D}^{-\frac{1}{2}} \bar{A} \bar{D}^{-\frac{1}{2}} H^{l-1} W^l), \quad (2)$$

$$\bar{A} = A + I_N, \quad (3)$$

$$\bar{D}_{ii} = \sum_j \bar{A}_{ij}. \quad (4)$$

where  $A$  is the adjacency matrix of the modelled undirected EEG electrodes graph,  $I_N$  is the identity matrix,  $\bar{D}$  is the degree matrix and  $W$  is a trainable weight matrix.  $\sigma(\cdot)$  denotes an activation function.

The model input the EEG features (PSD features) to the graph convolution layer, which can obtain the feature vectors on nodes that contain both spectral and spatial features. The RELU nonlinearity is used as in the graph convolution layer. We apply regularization on two fully connected layers with  $l1 = 0.01$ , and train the models using categorical cross-entropy loss. In order to understand the details of hyperparameters involved in the model, we list the configuration in Table II, where input is pre-processed data with PSD features.

TABLE II. SPECTRAL-SPATIAL MODEL STRUCTURE

	Output	Activation
Input	(30, 3)	
Graph convolution layer	(30, 128)	RELU
Flatten	3840 units	
Dense	(1, 512)	RELU
Dense	(1, 512)	RELU
Dense	(1, 2)	SOFTMAX

### E. Setting of baseline models

We test the subject-independent performance of our model on the prepared driving dataset. Logistic regression (LR) and support vector machine (SVM) are

used as baseline methods. These two methods are widely used traditional methods for EEG-based classification. Besides, since the deep learning models can have a larger capacity to store a large number of information of different subjects, deep learning models is expected to have a better performance than traditional machine learning methods. EEGNet [33], specially, is a state-of-the-art CNN model designed for EEG related signal processing, which can extract spatial feature by using depthwise-convolution. The hyperparameters setting of the baseline models is described as below:

LR: The model parameters of LR were optimized by batch gradient descent which was set to run for 100 iterations.

SVM: We employ the Bayesian optimization in Matlab to tune the SVM classifier automatically.

EEGNet: The default parameters set in [33] was used in the comparison. Both EEGNet-4.2 and EEGNet-8.2 were tested. The models were fit by minimizing the binary cross-entropy using Adam optimizer.

#### F. Model explainability and spatial localization of SA

Since the S-S model focus on the small areas in the brain and is based on the graph topologies of EEG channels, we employ the “nodes occlusion” method to interpret our S-S model, exploring the impact of different group of nodes on the graph topology. Nodes occlusion is similar to the “sequence dropout” method [29], which is to investigate the spatial localization of SA by omitting one node and observing the impact on the model’s output. We employ two rules to conduct the “node occlusion”. The first rule is that we explore the node-wise impact and obtain the individual impact of different nodes. The other one is that we divide the whole brain into three areas: left frontal region, right frontal region and the occipital region.

## IV. RESULTS

The whole experiment is conducted on the Windows 10 platform powered by an NVIDIA GeForce GTX 1080 graphics card. We make use of TensorFlow 2.1.0 to implement the model with python 3.7.7.

#### A. Comparison of spectral-spatial model and baseline models

We performed the leave-one-subject-out cross-validation for situation awareness classification. The accuracy of different methods is shown in Table III. From the comparison of the results, we can see that our spectral-spatial model performs better than other state-of-the-art methods.

We applied one-way ANOVA to analyse the significance of difference of models’ results. Significant difference in the mean accuracy of the five models ( $F_{(4,45)}, p < 0.001$ ) was observed.

#### B. Validation of the graph model of EEG channels

In order to better understand the importance and the validity of our modelled topological structure, we replace the modelled  $\{0, 1\}$  adjacency matrix with an identity matrix and a random symmetric matrix (the structure is an undirected graph). The results are obtained from the spectral-spatial model and shown in Table IV.

The model trained with both identity and random  $30 \times 30$  adjacency matrix does not have good performance, indicating the validity of the 1-step reachable adjacency matrix. The spatial information between nodes and corresponding 1-step neighbouring nodes can indeed help to improve the performance of the cross-subject SA recognition.

#### C. Model explainability and spatial localization of SA

Here we test the spatial localization of SA in the brain. The channels groups we set for each area of brain are shown in Table V, which were used to generate Figure 3 (b).

The nodes occlusion visualization method can help us to have a better understanding of the relationship between SA and our brain. The spatial localization results are shown in Figure 3. The intensity of nodes is negative related with the classification results. In our experiment, we obtain that the nodes “OZ, P4, CP4, FC3, F4” are top 5 that can better reflect the change of SA. However, most of the classification results are similar. Since the neighbouring channels can also contain the information of the centre node to some extent and the topology has a little change, the useful EEG channels cannot be clearly specified. The results of rule 2 can better show the localization of SA in the brain. The visualization of rule 2 presents that the occipital region has the best result among these three areas while the counterpart of the right frontal region is the worst. Three classification results are: 0.650 (left frontal region), 0.675 (right frontal region) and 0.606 (occipital region). The result of the occipital region which is far less than the others can better reflect the fatigue-related SA. The results of two rules is compatible with the previous investigation that the prefrontal, anterior cingulate, parietal, and visual regions are associated with SA [14].

## V. DISCUSSION

In this paper, we propose a S-S model for fatigue-related SA recognition from EEG data. The novelty of S-S model is that the graph convolutional layer is used to extract the spatial features for each EEG channel. Comparison results showed that the performance of our S-S model is better than other state-of-the-art models. From the analysis of spatial localization of SA, it demonstrated that the proposed S-S model can indeed learn useful features from the graph topology. However, the further study on specific learned feature is needed.

Regarding the recognition accuracy of different subjects, we can see that the results of subject 3 are below 50%. For subject-independent EEG-based mental state recognition, because of the individual difference on their EEG signal, the binary classification accuracy is not very high compared with the subject-dependent mental state recognition. This result also shows that the proposed S-S model contributes to improving the performance of cross-subject SA classifier, but the model still cannot extract better features that can overcome the difficulty of individual differences. For the problem, in next step, the use of eye movement signal could be helpful to improve the performance of our model, resulting from the strong relation between SA and subjects’ eye movement signal.

TABLE III. SITUATION AWARENESS CLASSIFICATION RESULTS OF LEAVE-ONE SUBJECT-OUT CROSS-VALIDATION TEST

Subject ID	LR	SVM	EEGNet-4.2	EEGNet-8.2	Spectral-spatial model
1	0.686	0.649	0.624	0.660	<b>0.739</b>
2	0.575	0.409	0.543	0.515	<b>0.591</b>
3	0.433	0.420	<b>0.489</b>	0.427	0.446
4	<b>0.682</b>	0.473	0.567	0.534	0.568
5	0.688	0.606	0.530	0.518	<b>0.741</b>
6	0.765	0.777	0.579	0.675	<b>0.813</b>
7	0.735	0.657	0.685	<b>0.774</b>	0.735
8	0.714	0.793	0.487	0.486	<b>0.814</b>
9	0.854	<b>0.861</b>	0.736	0.778	0.826
10	0.712	0.833	0.735	0.731	<b>0.917</b>
11	<b>0.628</b>	0.535	0.512	0.531	0.575
Average	0.679	0.638	0.590	0.603	<b>0.706</b>

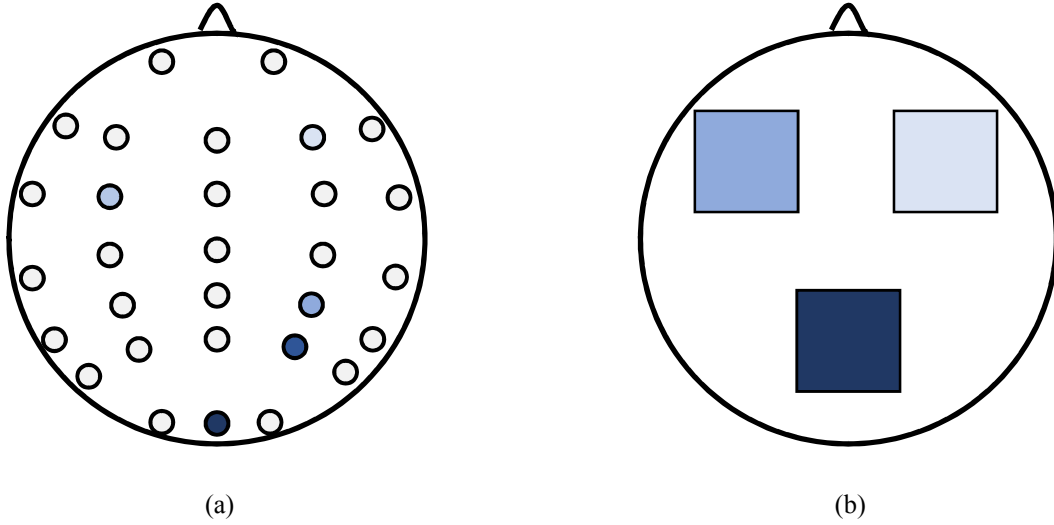


Figure 3. Spatial localization of SA in the brain. The intensity shows the negative impact of ignoring corresponding nodes on the model's output. The darker blue indicates the higher accuracy reduction. (a) The impact of all individual nodes on the model. (b) The impact of different brain areas on the model.

TABLE IV. CLASSIFICATION ACCURACY WITH DIFFERENT ADJACENCY MATRIX

Graph	Accuracy
Modelled $\{0, 1\}$ matrix	0.706
Identity	0.657
Random	0.639

TABLE V. CHANNEL GROUPS FOR DIFFERENT BRAIN AREAS

Area	Channels Group
Left frontal region	FP1, F7, F3, PT7, FC3, T3, C3, TP7, CP3
Right frontal region	FP2, F8, F4, FT8, FC4, T4, C4, TP8, CP4
Occipital region	T5, P3, P1, P4, T6, O1, OZ, O2

## VI. CONCLUSION

In this paper, we present a study of cross-subject fatigue-related situation awareness recognition. Firstly, the EEG channels are modelled into the topological structure and obtain the “EEG graph”. A  $\{0, 1\}$  adjacency matrix is obtained based on the physical distance between two EEG channels. Secondly, a spectral-spatial model is proposed to extract both spectral and spatial information in EEG channels. The PSD features are extracted. We employ the graph convolution operation to perform aggregation for each node, extracting spatial feature for each node. We conduct the experiment on a public EEG dataset to explore the subject-independent performance of the proposed model by using leave-one-subject-out cross-validation test. The S-S model achieves the best performance (70.6%) compared with four state-of-the-art methods: logistic regression (67.9%), support vector machine (63.8%), EEGNet-4.2 (59.0%) and EEGNet-8,2(60.3%). We also perform the “nodes occlusion” method to better understand the spatial localization of SA in the brain. The visualization results show that the occipital region plays an important role in SA recognition. The overall experiment results demonstrate the accuracy and utility of the model, which is a promising method for cross-subject situation awareness recognition. In the future, the temporal feature extraction can be performed based on spatial information, which shall lead to a good improvement.

## ACKNOWLEDGMENT

This research is supported by the National Research Foundation, Singapore under its International Research Centres in Singapore Funding Initiative. Any opinions, findings and conclusions or recommendations expressed in this material are those of the author(s) and do not reflect the views of National Research Foundation, Singapore.

## REFERENCES

- [1] L. Petersen, L. Robert, J. Yang, and D. Tilbury, "Situational awareness, driver's trust in automated driving systems and secondary task performance," *SAE International Journal of Connected and Autonomous Vehicles*, Forthcoming, 2019.
- [2] T. Vogelpohl, M. Kühn, T. Hummel, and M. Vollrath, "Asleep at the automated wheel—Sleepiness and fatigue during highly automated driving," *Accident Analysis & Prevention*, vol. 126, pp. 70-84, 2019/05/01/ 2019.
- [3] M. R. Endsley, "Measurement of situation awareness in dynamic systems," *Human factors*, vol. 37, no. 1, pp. 65-84, 1995.
- [4] T. Nguyen, C. P. Lim, N. D. Nguyen, L. Gordon-Brown, and S. Nahavandi, "A Review of Situation Awareness Assessment Approaches in Aviation Environments," *IEEE Systems Journal*, vol. 13, no. 3, pp. 3590-3603, 2019.
- [5] M. R. Endsley, "Situation awareness global assessment technique (SAGAT)," in *Proceedings of the IEEE 1988 national aerospace and electronics conference, 1988*, pp. 789-795: IEEE.
- [6] F. T. Durso, C. A. Hackworth, T. R. Truitt, J. Crutchfield, D. Nikolic, and C. A. Manning, "Situation awareness as a predictor of performance for en route air traffic controllers," *Air Traffic Control Quarterly*, vol. 6, no. 1, pp. 1-20, 1998.
- [7] J. Luo, Z. Feng, J. Zhang, and N. Lu, "Dynamic frequency feature selection based approach for classification of motor imageries," *Computers in biology and medicine*, vol. 75, pp. 45-53, 2016.
- [8] E. Salas, *Situational awareness*. Routledge, 2017.
- [9] J. Li, Z. Zhang, and H. He, "Hierarchical convolutional neural networks for EEG-based emotion recognition," *Cognitive Computation*, vol. 10, no. 2, pp. 368-380, 2018.
- [10] M. R. Endsley, "Supporting situation awareness in aviation systems," in *1997 IEEE International Conference on Systems, Man, and Cybernetics. Computational Cybernetics and Simulation, 1997*, vol. 5, pp. 4177-4181: IEEE.
- [11] M. R. Endsley, "Automation and situation awareness," *Automation and human performance: Theory and applications*, vol. 20, pp. 163-181, 1996.
- [12] Y. Liu, Z. Lan, J. Cui, O. Sourina, and W. Müller-Wittig, "EEG-Based Cross-Subject Mental Fatigue Recognition," in *2019 International Conference on Cyberworlds (CW)*, 2019, pp. 247-252: IEEE.
- [13] R. F. Rojas et al., "Encephalographic Assessment of Situation Awareness in Teleoperation of Human-Swarm Teaming," in *International Conference on Neural Information Processing*, 2019, pp. 530-539: Springer.
- [14] D. Catherwood et al., "Mapping brain activity during loss of situation awareness: an EEG investigation of a basis for top-down influence on perception," *Human factors*, vol. 56, no. 8, pp. 1428-1452, 2014.
- [15] L. G. Yeo et al., "Mobile EEG-based situation awareness recognition for air traffic controllers," in *2017 IEEE International Conference on Systems, Man, and Cybernetics (SMC)*, 2017, pp. 3030-3035: IEEE.
- [16] H. T. French, E. Clarke, D. Pomeroy, M. Seymour, and C. R. Clark, "Psycho-physiological measures of situation awareness," *Decision making in complex environments*, vol. 291, 2007.
- [17] C. Berka, D. J. Levendowski, G. Davis, M. Whitmoyer, K. Hale, and S. Fuchs, "Objective measures of situational awareness using neurophysiology technology," *Augmented Cognition: Past, Present and Future*, pp. 145-154, 2006.
- [18] M. A. Vidulich, M. Stratton, M. Crabtree, and G. Wilson, "Performance-based and physiological measures of situational awareness," *Aviation, space, and environmental medicine*, 1994.
- [19] P. Bashivan, I. Rish, M. Yeasin, and N. Codella, "Learning representations from EEG with deep recurrent-convolutional neural networks," *arXiv preprint arXiv:1511.06448*, 2015.
- [20] R. G. Hefron, B. J. Borghetti, J. C. Christensen, and C. M. S. Kabbani, "Deep long short-term memory structures model temporal dependencies improving cognitive workload estimation," *Pattern Recognition Letters*, vol. 94, pp. 96-104, 2017.
- [21] T. N. Kipf and M. Welling, "Semi-supervised classification with graph convolutional networks," *arXiv preprint arXiv:1609.02907*, 2016.
- [22] M. Defferrard, X. Bresson, and P. Vandergheynst, "Convolutional neural networks on graphs with fast localized spectral filtering," in *Advances in neural information processing systems*, 2016, pp. 3844-3852.
- [23] L. Zhao et al., "T-gcn: A temporal graph convolutional network for traffic prediction," *IEEE Transactions on Intelligent Transportation Systems*, 2019.
- [24] F. Scarselli, M. Gori, A. C. Tsoi, M. Hagenbuchner, and G. Monfardini, "The graph neural network model," *IEEE Transactions on Neural Networks*, vol. 20, no. 1, pp. 61-80, 2008.
- [25] F. R. Chung and F. C. Graham, *Spectral graph theory* (no. 92). American Mathematical Soc., 1997.
- [26] P. Zhong, D. Wang, and C. Miao, "EEG-Based Emotion Recognition Using Regularized Graph Neural Networks," *arXiv preprint arXiv:1907.07835*, 2019.
- [27] R. Salvador, J. Suckling, M. R. Coleman, J. D. Pickard, D. Menon, and E. Bullmore, "Neurophysiological architecture of functional magnetic resonance images of human brain," *Cerebral cortex*, vol. 15, no. 9, pp. 1332-1342, 2005.
- [28] Z. Wang, Y. Tong, and X. Heng, "Phase-Locking Value Based Graph Convolutional Neural Networks for Emotion Recognition," *IEEE Access*, vol. 7, pp. 93711-93722, 2019.

- [29] I. Covert et al., "Temporal Graph Convolutional Networks for Automatic Seizure Detection," arXiv preprint arXiv:1905.01375, 2019.
- [30] Z. Cao, C.-H. Chuang, J.-K. King, and C.-T. Lin, "Multi-channel EEG recordings during a sustained-attention driving task," *Scientific data*, vol. 6, no. 1, pp. 1-8, 2019.
- [31] W. Hamilton, Z. Ying, and J. Leskovec, "Inductive representation learning on large graphs," in *Advances in neural information processing systems*, 2017, pp. 1024-1034.
- [32] K. Xu, W. Hu, J. Leskovec, and S. Jegelka, "How powerful are graph neural networks?," arXiv preprint arXiv:1810.00826, 2018.
- [33] V. J. Lawhern, A. J. Solon, N. R. Waytowich, S. M. Gordon, C. P. Hung, and B. J. Lance, "EEGNet: a compact convolutional neural network for EEG-based brain-computer interfaces," *Journal of neural engineering*, vol. 15, no. 5, p. 056013, 2018.